Annals of Diagnostic Pathology 43 (2019) 151403

Contents lists available at ScienceDirect

Annals of Diagnostic Pathology

journal homepage: www.elsevier.com/locate/anndiagpath

Renal crystal-storing histiocytosis involving glomeruli – A comprehensive clinicopathologic analysis

Rajib K. Gupta[1], Avi Z. Rosenberg, Serena M. Bagnasco, Lois J. Arend*

Renal Pathology, Department of Pathology, Johns Hopkins University and Johns Hopkins Hospital, Baltimore, MD 21287, USA

ARTICLE INFO

Keywords:
Crystal-storing histiocytosis (CSH)
Multiple myeloma
Plasma cell dyscrasia
Dysproteinemia
Kidney biopsy

ABSTRACT

Crystal-storing histiocytosis (CSH) is a rare manifestation of monoclonal gammopathy in which histiocytes containing monoclonal proteins in their cytoplasm are found in various organs of the body including the kidney. Within the kidney, these monoclonal crystal-laden histiocytes have been described to occur in the interstitium (most commonly) or in the glomerular mesangium. CSH within glomerular capillary loops has rarely been reported. We describe three cases of CSH primarily affecting the glomerular capillaries and review the literature of CSH in general. Twenty cases of CSH involving the kidney are present in the literature; three describe CSH in glomeruli, only one of which showed histiocytes predominantly in glomerular capillary loops, while 15 had predominantly or solely interstitial CSH. Most cases involve IgG kappa crystals with only one case involving lambda light chain. Patients with CSH predominantly involving the glomerular capillaries showed a trend toward lower serum creatinine and proteinuria at presentation, and several patients with CSH lacked a definitive diagnosis of a monoclonal gammopathy at the time of diagnosis, emphasizing the role that kidney biopsy and particularly electron microscopy play in diagnosis of this entity.

1. Introduction

Multiple myeloma (including monoclonal gammopathy of uncertain significance [MGUS]) and various B-cell lymphoproliferative disorders (mostly low-grade) often involve the kidney and result in a variety of morphologic manifestations which can be subtyped based on light microscopic or ultrastructural features. These disorders usually show laboratory features of monoclonal gammopathy characterized by an underlying plasma cell dyscrasia or a low-grade B-cell lymphoma, positive monoclonal spike (M-spike) on immunoelectrophoresis (usually IgG or IgM, rarely IgA), and elevated free kappa or lambda light chain [1]. Often, kidney biopsy for renal dysfunction and/or proteinuria is the first indication of a monoclonal process. Morphologically, there is deposition of monotypic kappa or lambda light chains or heavy chains (or both) in the kidney, sometimes involving more than one compartment (Fig. 1). Although many of the different morphologic entities are often suspected by light microscopy, electron microscopy is the gold standard by which these various monoclonal proteins are ultimately diagnosed and classified.

Crystal-bearing or crystal-storing histiocytosis (CSH) is a rare morphologic manifestation of monoclonal gammopathy in which monoclonal crystals, usually belonging to kappa subtype and having various geometric shapes, collect within histiocytes that, *via* systemic circulation, end up in various organs [2-9]. In the kidney, such histiocytes have been historically described in the renal interstitium or occasionally in the mesangium [5-8,10-23]. Crystal-storing histiocytes involving the glomerular capillary loops have rarely been reported [22].

We report several cases from our institution with striking gross, light microscopic, and ultrastructural features, and extensively review the existing literature on renal CSH, correlating histology with clinical features.

2. Materials and methods

With IRB approval, computerized records of native kidney biopsies received from 1/1/1994 to 12/31/2017 were searched using terms monoclonal or gammopathy (650 cases out of 23,385), with subsequent search of these results for crystal or histiocytosis. Four cases (< 0.02%) diagnosed as crystal-storing histiocytosis were identified. One of these was an initial biopsy on the patient presented here as Case 2 who was subsequently re-biopsied. The demographic and clinical information

* Corresponding author at: Johns Hopkins University School of Medicine, Department of Pathology, Johns Hopkins Hospital, 600 N Wolfe Street, Pathology 709, Baltimore, MD 21287, USA.
E-mail address: ljarend@jhu.edu (L.J. Arend).
[1] Present address: Division of Renal Pathology, Department of Pathology, SUNY Upstate Medical University, Syracuse, NY 13210, USA.

https://doi.org/10.1016/j.anndiagpath.2019.151403

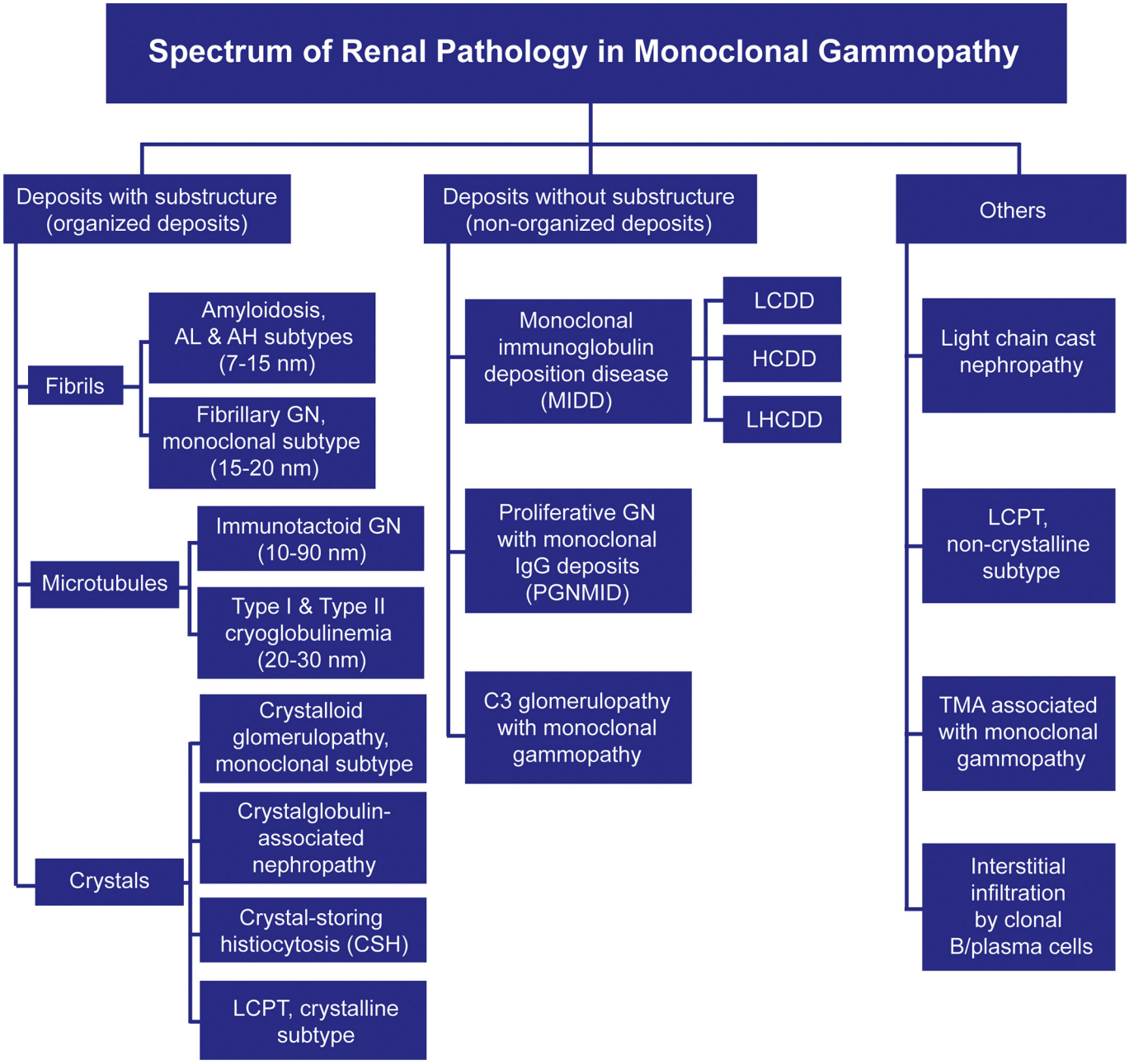

Fig. 1. The current spectrum of pathologic entities associated with monoclonal gammopathy in renal disease.

provided at the time of biopsy and afterwards was recorded including age at biopsy, gender, race, relevant past medical history, serum creatinine, urinalysis and urine protein quantification, pertinent laboratory tests and other pathology diagnoses, clinical course and follow up (when documented).

2.1. Biopsies

Native kidney biopsies were processed for light microscopy, immunofluorescence, and electron microscopy as per standard protocol for diagnostic evaluation. Biopsies and pathologic reports were reviewed by two nephropathologists (RKG and LJA). Immunohistochemical staining on paraffin embedded tissue was performed for CD68 (Ventana 790-2931), CD163 (Novacastra NCL-CD163), CD138 (Ventana 760-4248), kappa light chain (Dako A0191), lambda light chain (Dako A0193), S100 (Ventana 790-2914), and CD1a (Novacastra IM1590) using standard immunohistochemical methods.

2.2. Immunoelectron microscopy

Immunogold electron microscopy was performed for kappa and lambda light chains as follows. Biopsy tissue was fixed with 3% glutaraldehyde in 0.1 M phosphate buffer, pH 7.3 overnight at 4C. Tissue was washed in the same buffer for 15 min, 3 times, prior to secondary fixation with 1% osmium tetroxide in 0.1 M phosphate buffer for 1 h at room temperature. The tissues were dehydrated using a graded ethanol series, transitioned through toluene, infiltrated and embedded with Poly/Bed 812 epoxy resin, and polymerized overnight at 60C. Areas of interest for immunoelectron microscopy (IEM) were selected from thick sections (1 μm) stained with Toluidine blue. Thin sections (100 nm) were cut with a diamond knife (DIATOME) and placed on 200 mesh nickel grids for post-embed immunogold staining.

Prior to immunostaining, antibody binding sites were unmasked by treating the sections with 4% sodium metaperiodate for 30 min at room temperature. After 3 rinses in deionized water for 1 min each, non-

specific binding sites were blocked by treating with 1% bovine serum albumin (BSA) in phosphate buffered saline (PBS) for 10 min at room temperature.

Rabbit polyclonal antibodies (IgG) against human kappa (polyclonal rabbit anti-human kappa light chain, Dako A0191) or lambda (polyclonal rabbit anti-human lambda light chain, Dako A0193) light chains were used. The grids were floated on drops of primary antibody diluted in 0.5% BSA/PBS and incubated overnight at 4C. Omission of primary antibody served as method control. Parallel control grids were floated on drops of 0.5% BSA/PBS only. The next day, after rinsing sections in 0.5% BSA/PBS for 5 min, 3 times, the sections were incubated with polyclonal goat affinity purified anti-rabbit IgG (H + L) conjugated to 10 nm gold particles (Cytodiagnostics AC-10-01) for 1 h at room temperature. The sections were washed in PBS for 5 min, 3 times, stabilized by post fixation in 3% glutaraldehyde in PBS for 3 min, rinsed in deionized water and air-dried on filter paper. Some grids were post-stained with uranyl acetate and lead citrate to correlate gold labeling with ultrastructure.

The grids were placed into a JEOL1400 Plus transmission electron microscope (TEM) equipped with a lanthanum hexaboride cathode operating at 80 kV accelerating voltage. The acquisition of electron micrographs at various magnifications was performed using a QUEMESA 11 megapixel bottom-mounted CCD TEM camera system (Olympus Soft Imaging Solutions).

2.3. Statistical analysis

Statistical analysis was performed in GraphPad (LaJolla, CA) using unpaired *t*-test.

3. Results

3.1. Case 1

A 71-year old male presented with nephrotic-range proteinuria of 3.6 g/day and serum creatinine of 1.18 mg/dL. He had a history of B-cell lymphoproliferative disorder and Waldenstrom macroglobulinemia for 17 years, for which he had received chemotherapy. He had disease recurrence which required a splenectomy and additional cycles of chemotherapy with a variety of regimens. A previous kidney biopsy performed at an outside hospital 5 years prior to the current presentation had shown kappa-positive crystal-containing interstitial macrophages. Currently, his serum showed monoclonal IgM protein with elevated free kappa light chain and a kappa/lambda ratio of 25. A second kidney biopsy was performed.

The appearance of the fresh biopsy core using a dissecting microscope was distinctly abnormal and showed hypertrophic solid-appearing glomeruli (Fig. 2a). On light microscopy, the biopsy contained cortex and medulla with up to 24 glomeruli per section, of which 3–4 glomeruli were globally sclerosed. The remaining glomeruli showed a striking appearance with dilated capillary loops filled with large histiocyte-like cells containing eosinophilic cytoplasmic globules on H&E (Fig. 2b) that were strongly fuchsinophilic on trichrome stain (Fig. 2c). A few of these cells were also found scattered in the interstitium. The tubules showed focal injury in the form of tubular cell vacuolization, flattening of the epithelium and apical blebbing, along with a deep eosinophilic appearance of the tubular epithelia. The interstitium showed focal edema and patchy interstitial inflammatory infiltrates composed of lymphocytes, plasma cells, and prominent eosinophils. Arteries up to arcuate size were present, many of which showed moderate to severe fibrointimal thickening. Immunohistochemical staining for CD68 highlighted cells within the glomeruli and in the interstitium (Fig. 2d). Immunohistochemistry for kappa and lambda light chains showed the histiocytic cells to have restricted staining for kappa (Fig. 2e & f). Direct immunofluorescence on frozen tissue revealed that the histiocytes within the capillaries were positive for kappa light chain (2 +) and IgM (0–1 +), and were negative for lambda, IgG, IgA, C3, and C1q (Fig. 2g & h).

Toluidine blue stained thick sections highlighted the intracytoplasmic globules within the histiocytes (Fig. 2i). Ultrastructurally, the glomerular capillaries were occluded and distended by large cells with electron-dense polygonal crystalline inclusions in their cytoplasm (Fig. 2j & k). A few of these crystals were seen within the cytoplasm of glomerular endothelial cells and others were seen apparently representing circulating monoclonal protein free within the lumina of peritubular capillaries (some being engulfed by macrophages; Fig. 2l). Few proximal tubular cells also showed cytoplasmic crystalline inclusions. On higher ultrastructural magnification the crystals revealed a lattice substructure. The glomerular basement membranes were irregularly thickened but did not show crystalline, granular, or powdery electron-dense deposits. No electron-dense deposits were evident along the tubular basement membranes. The podocytes showed segmental effacement of up to 60% of the capillary surface. Immunoelectron microscopy using kappa and lambda gold particles confirmed kappa restriction of the crystals. Final diagnosis was rendered as crystal-storing histiocytosis, kappa light chain-restricted, with dominant glomerular involvement.

3.2. Case 2

A 67-year old male with a history of diabetes, hypertension, obesity, and myelodysplastic syndrome was diagnosed several years prior to the current presentation with ANCA-negative pauci-immune glomerulonephritis with arteritis and features of thrombotic microangiopathy. He developed acute kidney injury five years later, with a serum creatinine of 4.6 mg/dL, which responded to IV fluids and was presumed secondary to use of non-steroidal anti-inflammatory drug (NSAID). Seven months later he developed a rash, bilateral lower extremity edema, anemia, low platelets, and increase in serum creatinine from 1.3 mg/dL to 1.8 mg/dL. Serum protein electrophoresis revealed an IgG kappa monoclonal gammopathy and cryoglobulin screen was trace positive. There were no radiologic or clinical signs of frank myeloma. A kidney biopsy was performed at that time, and a second biopsy 2 months later for further worsening of renal function (serum creatinine 2.7 mg/dL).

Most glomeruli had a membranoproliferative glomerulonephritis (MPGN) appearance with histiocyte-like cells within capillary loops containing small eosinophilic droplets or globules on H&E (Fig. 3a) and double contours of the capillary walls on silver stain (Fig. 3b). There was approximately 30–40% tubular atrophy and interstitial fibrosis, with preserved tubules showing cytoplasmic vacuolization, apical blebbing and thinning. On immunohistochemistry, the histiocytes were positive for the monocyte markers CD68 and CD163 (Fig. 3c) and for kappa, and were negative for CD138, S100, CD1a and lambda. Direct immunofluorescence studies showed 3 + focal globular and segmental staining in mesangium and capillaries for IgG, kappa, and C3. Toluidine blue-stained thick sections highlighted the intra-histiocytic globules. Ultrastructurally, many of the glomerular capillary loops showed marginating cells with indented nuclei containing numerous cytoplasmic electron-dense round to oval crystalloid structures with smooth outer contours (Fig. 3d). In a few glomeruli, these oval crystals were seen within the cytoplasm of endothelial cells; rare foci also showed more conventional granular subendothelial electron-dense deposits (Fig. 3e). Immunoelectron microscopy showed particulate kappa gold staining of the crystals, and no staining for lambda (Fig. 3f). Final diagnosis was MPGN due to IgG kappa crystal-storing histiocytosis.

3.3. Case 3

A 74-year old male developed acute renal failure, with an increase in serum creatinine to 3.5 mg/dL from a baseline of 0.5 mg/dL. Proteinuria of 2 g per day was detected. Testing for ANCA, anti-GBM antibody, Hepatitis B, and Hepatitis C was negative. A kappa

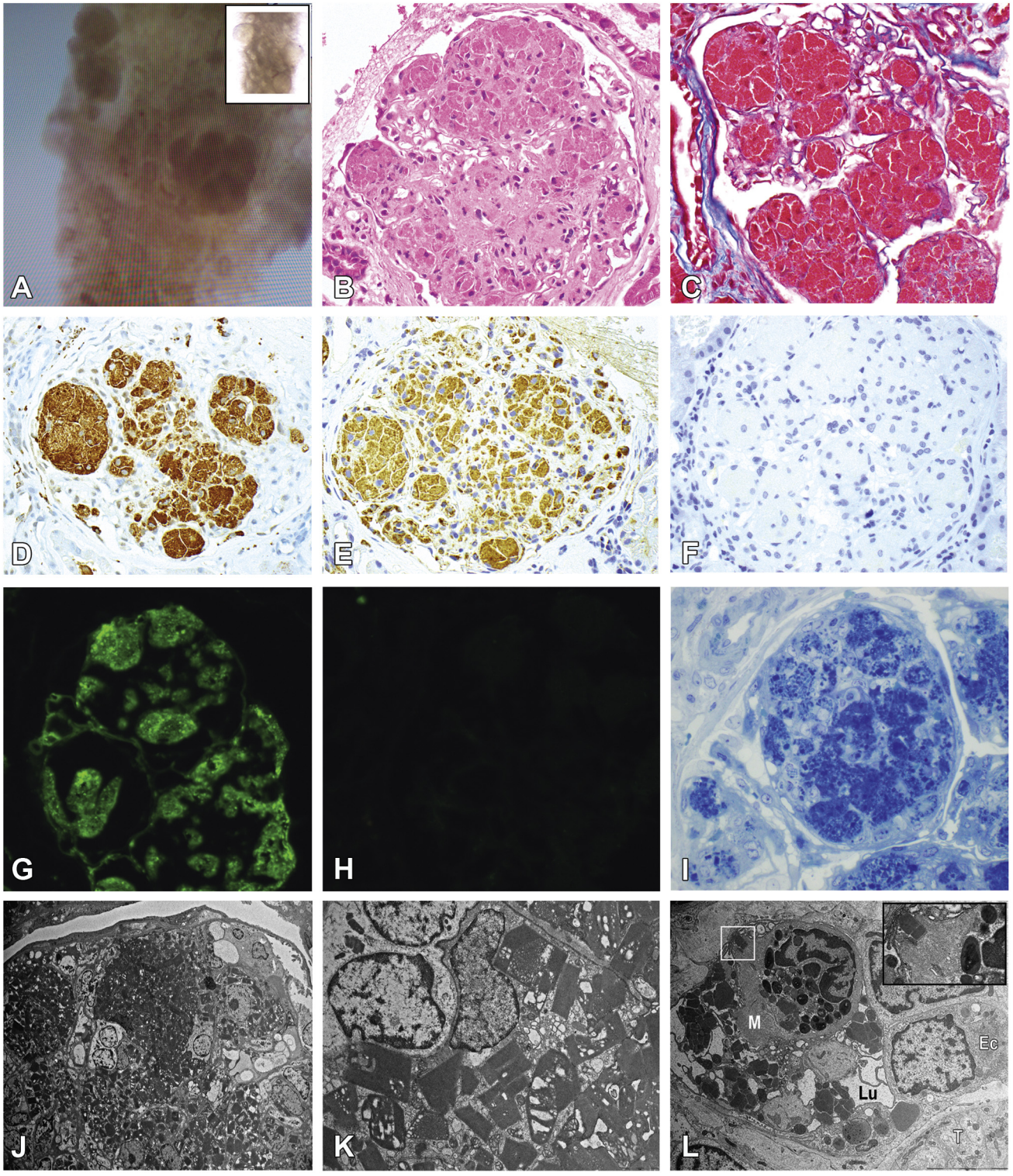

Fig. 2. Biopsy images from Case 1: (a) gross picture of the frozen biopsy core under the dissecting microscope showing a large hypertrophic, solid-appearing glomerulus (inset: gross picture of a kidney biopsy core of an unrelated case from our renal lab for comparison, showing normal-appearing glomeruli). (b) Hematoxylin and eosin (H&E) image of a representative glomerulus showing enlarged, slightly lobulated glomerulus with capillary loops being almost completely occluded with histiocyte-like cells having bright eosinophilic material in their cytoplasm (original magnification 400×); (c) Masson trichrome stain showing an enlarged glomerulus with bright fuchsinophilic crystals within the histiocytes (original magnification 400×). (d) CD68 immunohistochemical stain highlighting the histiocytes within the capillary loops (original magnification 400×). (e and f) Immunohistochemistry for kappa and lambda light chains, respectively, show strong kappa staining of the crystals, and no staining for lambda within the glomerulus (original magnification 400×). (g and h) Direct immunofluorescence shows bright staining for kappa and near-negative staining for lambda. (i) Thick section stained with toluidine blue shows prominent granular staining of the crystals within a representative glomerulus (original magnification 400×). (j) Electron microscopic (EM) view of a glomerular tuft with most of capillary loops filled with hexagonal crystals of varying sizes (magnification 10,000×). (k) EM image of the same glomerular tuft as in j at a higher power showing a crystal-laden macrophage (magnification 50,000×). (l) EM image of a peritubular capillary lined by endothelial cells (E) with several free hexagonal crystals within the lumen (Lu), and a monocyte-macrophage (M) at one corner within the lumen in the process of engulfing a crystal, a tubule (T) can be seen at one edge (magnification 50,000×), inset: higher magnification of the macrophage engulfing the crystal, (magnification 80,000×).

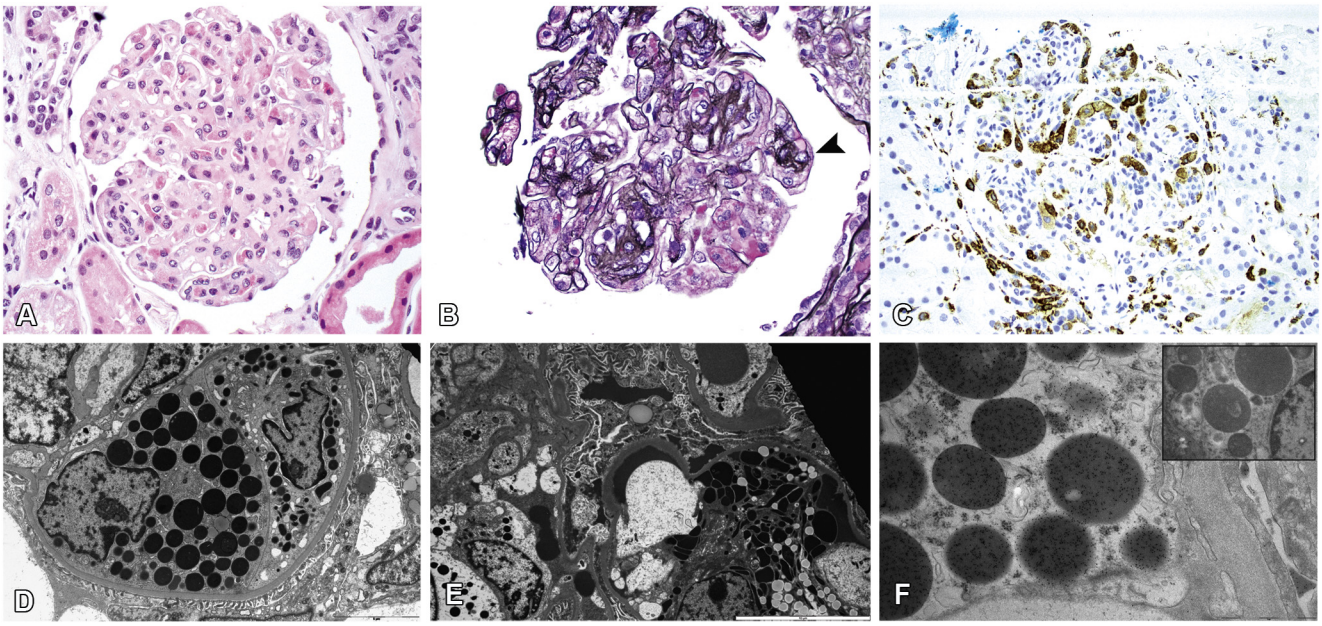

Fig. 3. Biopsy images from Case 2: (a) H&E image of a representative slightly enlarged glomerulus having a membranoproliferative glomerulonephritis (MPGN)-like appearance and showing partial occlusion of many capillary loops with histiocyte-like cells having an eccentric nucleus and bright eosinophilic granular cytoplasm (original magnification 400×). (b) Glomerulus showing distinct double contours (black arrowhead) of capillary walls (original magnification 400×). (c) CD163 immunostain highlighting the histiocytes within the capillary loops (original magnification 400×). (d) EM shows spherical electron-dense crystals within the cytoplasm of a histiocyte having an eccentric nucleus (magnification 50,000×). (e) EM of a glomerulus with granular mesangial and subendothelial electron-dense deposits (magnification 40,000×). (f) Immunoelectron microscopy image showing a glomerulus with kappa gold particles labeling the spherical crystals (magnification 50,000×). Inset: EM image showing absence of staining of the same crystals by lambda gold particles (magnification 50,000×).

monoclonal spike was identified, and MGUS was suspected. A kidney biopsy was performed.

Most of the glomeruli had an MPGN appearance with lobulation, hypercellularity, focal cellular interpositioning and double contours, and segmental intra-capillary histiocytes (Fig. 4a & b). As in the previous cases, the histiocytes showed strong fuchsinophilic staining of their cytoplasm on trichrome stain (Fig. 4c). Several intratubular proteinaceous casts were identified without definite fracturing or cellular reaction. Intra-capillary CD68-positive histiocytes were seen having globular cytoplasmic material which was positive only for kappa (Fig. 4d–f). Many of the tubular casts also stained strongly for kappa. A few interstitial CD68-positive histiocytes were also noted. Direct immunofluorescence showed globular endocapillary staining for IgG (3+) and granular mesangial C3 (3+); casts stained more intensely for kappa (3+) as compared to lambda (1+). Toluidine blue-stained sections highlighted the histiocytic globules within the glomerular capillaries (Fig. 4g). Ultrastructural examination revealed extensive glomerular basement membrane and capillary wall duplication with cellular interposition. Also seen was segmental occlusion of capillary lumina by cells with eccentric curved nuclei filled with cytoplasmic globular or ovoid electron-dense crystalloid bodies, many of which were also seen within the cytoplasm of endothelial cells (Fig. 4h). Sparse subepithelial and focal subendothelial granular electron-dense deposits were also noted (Fig. 4i). Podocyte foot processes were diffusely effaced. Final diagnosis was MPGN with IgG-kappa crystal-storing histiocytosis, associated with acute tubular injury. A comprehensive investigation revealed that the patient had multiple myeloma.

3.4. Literature review and clinicopathologic correlation

In our review of the literature on CSH involving the kidney, 20 cases were identified since 1978 (Table 1). Five of the cases [5-8,11] were autopsies where kidney involvement by systemic CSH was suspected antemortem but was only proven on postmortem histopathology. On average, time to death from all causes after diagnosis was 4.5 years in the nine cases in which the patient had died at the time of reporting (range: 4 months to 25 years). There is a clear male predominance in renal CSH (18 males, 4 females) with a mean age at diagnosis of 60 years (range: 41 to 74 years). All patients with predominant glomerular capillary involvement were male (with the possible exception of Case #22, a female patient in whom the intraglomerular location was not specified). Serum creatinine at presentation was 5.01 ± 4.43 mg/dL (average ± SD) in patients with interstitial involvement only and 2.38 ± 1.12 mg/dL in those with predominantly glomerular involvement by CSH ($p = 0.22$). Where 24-hour urine protein was reported, the average proteinuria in patients with interstitial-only involvement was 4.62 ± 7.68 g/day and 2.36 ± 1.27 g/day in those with predominantly glomerular involvement ($p = 0.54$). Seventeen of the patients had either overt myeloma or MGUS, with one case having additional type 1 cryoglobulinemia [22]. In addition, two cases (including one of our own) had a history of lymphoplasmacytic lymphoma [11], one had a history of low-grade B-cell lymphoproliferative disorder, type unspecified [12], and one was diagnosed with diffuse large B-cell lymphoma a few months after the kidney biopsy [20]. Regarding light chain type, kappa was overwhelmingly the predominant light chain, with only one case showing IgM lambda protein [12]. Overall, IgG kappa was found to be the most common monoclonal protein (11 cases), along with 2 cases of IgM kappa, 2 cases of IgA kappa, one case of IgD kappa, and 3 cases having only monoclonal kappa light chain. As the table shows, the crystal-laden histiocytes were found most commonly in the interstitium; only a single journal image [21] and a case report [22] describe these histiocytes within the glomerular tuft, with only the published image mentioning it as occurring within the glomerular capillary loops (the first of two biopsies from Case 2). In three cases, CSH was reported as the sole renal pathology finding [11,12,18], while in the majority of cases (78.3%) at least one other manifestation of a monoclonal process co-existed with renal CSH. Twelve of these included LCPT, seven showed crystalloid glomerulopathy, and five had associated LCCN. Interestingly, two cases described extra-renal amyloid deposition as a co-existing process. Overall, nine cases (39.1%) showed

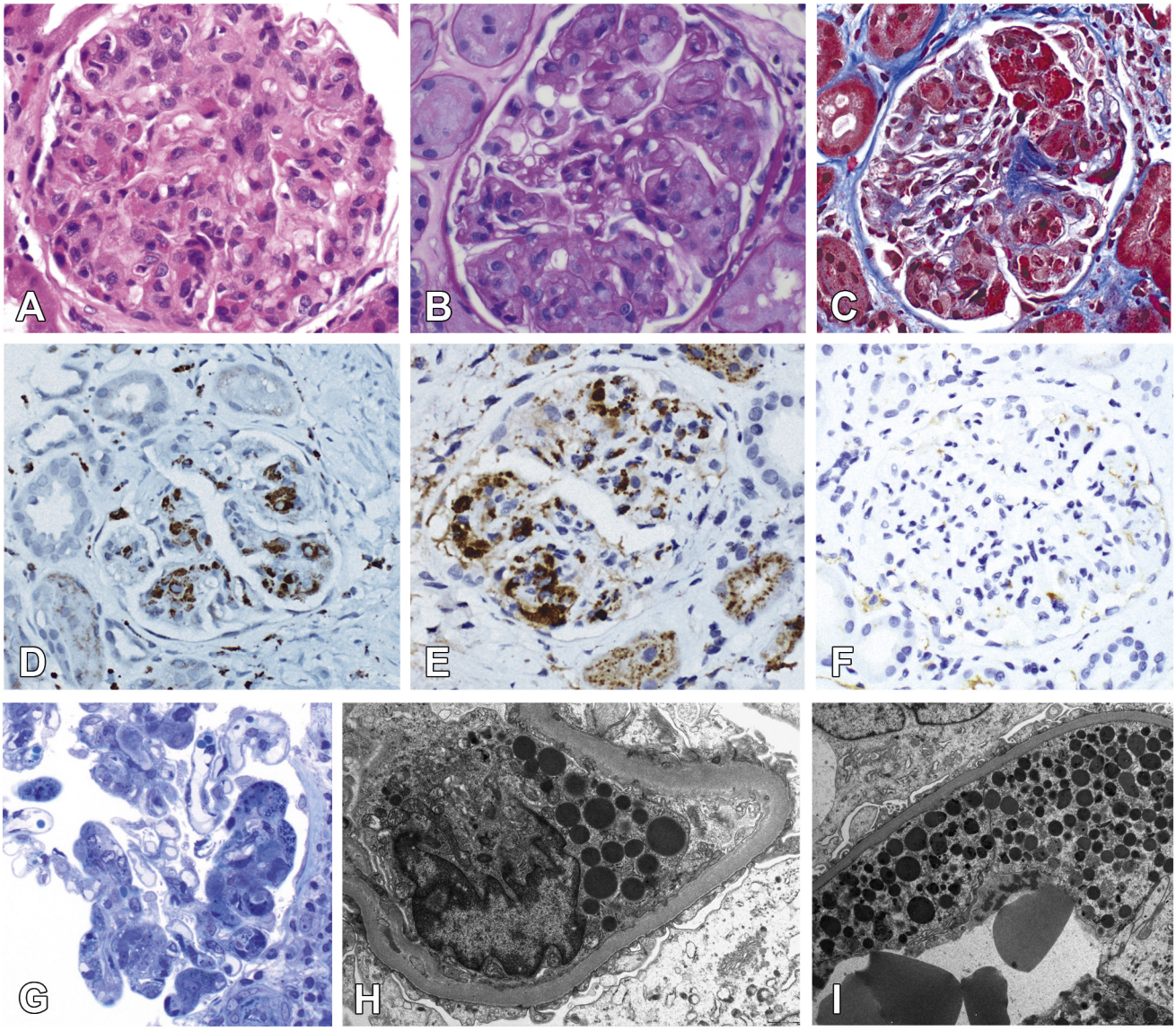

Fig. 4. Biopsy images from Case 3: (a) H&E image of a representative glomerulus having an MPGN appearance and scattered histiocyte-like cells with eosinophilic cytoplasm within many of its capillary loops (original magnification 400×). (b) PAS stain showing the histiocytes with pale foamy cytoplasm occluding the capillary loops within a glomerulus (original magnification 400×). (c) A Masson trichrome stain showing a similar glomerulus with histiocytes with bright fuchsinophilic material within the capillary loops (original magnification 400×). (d) CD68 immunostain highlighting the histiocytes in the glomerulus (original magnification 400×). (e and f) Kappa (e) and lambda (f) immunostains respectively show positive and negative staining of the glomerular crystals (original magnification 200×). (g) Thick section stained with toluidine blue showing segmental granular staining of the crystals within few of the capillary loops (original magnification 400×). (h) EM view of a macrophage cell almost occluding a capillary loop with several oval electron-dense crystals within its cytoplasm (magnification 50,000×). (i) An endothelial cell lining a capillary loop filled with the same oval electron-dense crystals (magnification 50,000×).

renal involvement by more than one additional manifestation, involving glomeruli, tubules, and interstitium. Involvement of renal vessels has not been described.

4. Discussion

Plasma cell dyscrasias and chronic B-cell lymphoproliferative disorders often result in monoclonal protein deposition (either kappa or lambda light chains or heavy chains) in different compartments of the kidney as various light microscopic and ultrastructural entities falling under the umbrella of monoclonal gammopathy-associated renal pathology. While cast nephropathy is still the most common pathology occurring in the kidney in such circumstances, monoclonal deposits with other morphologic forms have also been described and are often best seen ultrastructurally. These deposits seen by electron microscopy (EM), usually either have a substructure (fibrils, crystals, or microtubules) or are in the form of amorphous powdery deposits along glomerular or tubular basement membranes. Monoclonal crystals can take either of the following forms – (a) crystals within one or more cell types of the kidney which may be glomerular (mesangial cell and visceral epithelial cell) and/or extra-glomerular (usually proximal tubular epithelial cell), (b) extracellular crystals within glomerular capillary loops or within interstitial vessel lumina, and (c) infiltration of crystal-bearing histiocytes (Fig. 5).

Crystal-storing histiocytosis (CSH) is a rare pathologic variant of monoclonal protein-associated disease in which histiocytes containing monoclonal crystals in their cytoplasm are found in single or multiple organs of the body such as bone marrow, lungs, liver, stomach, spleen, kidney, skin, and cornea. These histiocytes have also been referred to as pseudo-pseudo-Gaucher cells (PPGC) in past literature to distinguish

Table 1
Clinical and pathologic features of patients with kidney involvement by CSH.

Case #	Age	Gender	Serum creatinine (mg/dL)	Urine protein[a]	Monoclonal protein	Associated hematologic process	Outcome	Location of crystal-storing histiocytes	Crystal configuration	Co-existing monoclonal associated pathology
1. Case 1	71	M	1.2	3.6	IgM kappa	LPL (WM)	DOD	I, G-Cl	Rh	CrG, LCPT
2. Case 2[b]	67	M	2.7	3–3.5	IgG kappa	MGUS	Died, ileus and liver failure, 4 months	G-Cl	O	CrG
3. Case 3	74	M	3.5	2.0	IgG kappa	MM	Stable, s/p CTX and hemodialysis	G-Cl	O	CrG
4. Terashima et al. 1978 [6][c]	58	M	2.5	0.5–1.0 g/dL	Kappa	MGUS	DOD, 3 years	I	Rh, N	LCPT, LCCN
5. Takahashi et al. 1987 [7][c]	60	M	N/A	N/A	IgA kappa	MM	DOD, 3 years, 9 months	I, G (site unspecified)	Rh, Rt, N	ERA
6. Carstens et al. 1989 [10]	57	M	3.2	2.0	IgG kappa	MM	Died, GI hemorrhage, 1.5 years	I	N, Rh	CrG, LCPT, ERA
7.Yamamoto et al. 1991 [8][c]	71	M	1.2	N/A	IgG kappa	MM	Died, sepsis, 4 years, 3 months	I	Rh	CrG, LCPT, LCCN
8. Garcia et al. 1998 [11][c]	44	M	N/A	N/A	IgG kappa	LPL	DOD, 1 yr	I	Rt, N	None
9. Sethi et al. 2002 [12]	58	M	3.3	0.5	IgM lambda	LGBLD	Stable, s/p CTX	G-M	Rh, Rt, N	None
10. Lebeau et al. 2002 [5][c]	73	M	N/A	N/A	IgA kappa	MM	Died, sepsis, 7 months	N/A	Rh, Rt	N/A
11.Tomioka et al. 2004 [13]	46	F	2.5	1.9	IgG kappa	MM	Stable, s/p CTX and SCT	I	Rh, O	CrG, LCPT, LCCN
12. Papla et al. 2004 [14]	51	M	N/A	N/A	IgG kappa	MM	DOD, lung cancer, 1 year	I	Rh	CrG, LCPT
13. Keller et al. 2005 [15]	56	M	14.5	0.5 g/dL	IgG kappa	MM	Stable, s/p CTX and SCT	I	N	CrG, LCPT
14. Tholouli et al. 2005 [16]	62	F	N/A	N/A	IgG kappa	MM	Stable, s/p CTX	I	Rh	LCPT
15. Stokes et al. 2006 [17]	41	M	4.2	20.2	IgD kappa	MM	Stable s/p CTX and SCT	I	Rh, N	LCPT, LCCN
16. Pitman et al. 2006 [18]	70	F	2.8	N/A	Kappa	MGUS (probable)	N/A	I	N/A	None
17. Farooq et al. 2009 [19]	66	M	2.5	0.05 g/dL	IgG kappa	MM	Stable, s/p CTX and SCT	N/A	N/A	LCPT
18–20. El Hamel et al. 2010 [20]	52	M	2.9	0.29	IgM kappa	MGUS	Died, sepsis, 25 years	I	N	LCPT
	70	M	2.4	0.8	IgM kappa	DLBCL (diagnosed 2 months after biopsy)	Died, sepsis after 6 courses of CTX	I	N, O	LCPT
	65	M	6.3	2.5	IgG kappa	MGUS	Stable on hemodialysis	I	N/A	N/A
21. Shah et al. 2016 [21]	67	M	1.8	3.1	IgG kappa	MGUS	Died, ileus and liver failure, 4 months	G-Cl	O	CrG
22. Hoelbeek et al. 2016 [22]	62	F	1.2	2.2	IgG kappa	Type 1 cryoglobulinemia associated with MGUS	Stable, s/p CTX and SCT	G (site unspecified)	N, Rh	CrG
23. Wu et al. 2017 [23]	48	M	12.6	N/A	Kappa	MM	Stable on hemodialysis, s/p CTX	I	Rh, N	LCPT, LCCN

Abbreviations: CSH, crystal-storing histiocytosis; LPL, lymphoplasmacytic lymphoma; WM, Waldenstrom macroglobulinemia; MGUS, monoclonal gammopathy of undetermined significance; MM, multiple myeloma; LGBLD, low-grade B-cell lymphoproliferative disorder; LCPT, light chain proximal tubulopathy, crystalline subtype; LCCN, light chain cast nephropathy; CrG, crystalloid glomerulopathy (includes crystals within podocytes or endothelial cells); ERA, extra-renal amyloidosis; DOD, died of disease; CTX, chemotherapy; SCT, stem cell transplant; N/A, not available; I, interstitial; G-M, glomerulus – mesangial; G-Cl, glomerulus – capillary loops; Rh, rhomboid or hexagonal; O, oval or globular; Rt, rectangular; N, needle- or rod-shaped.

[a] Proteinuria presented as grams/day, unless otherwise specified.

[b] The patient was biopsied twice, the first biopsy (Case 21) was published as an image by Shah et al. [21].

[c] Autopsy diagnosis of renal CSH.

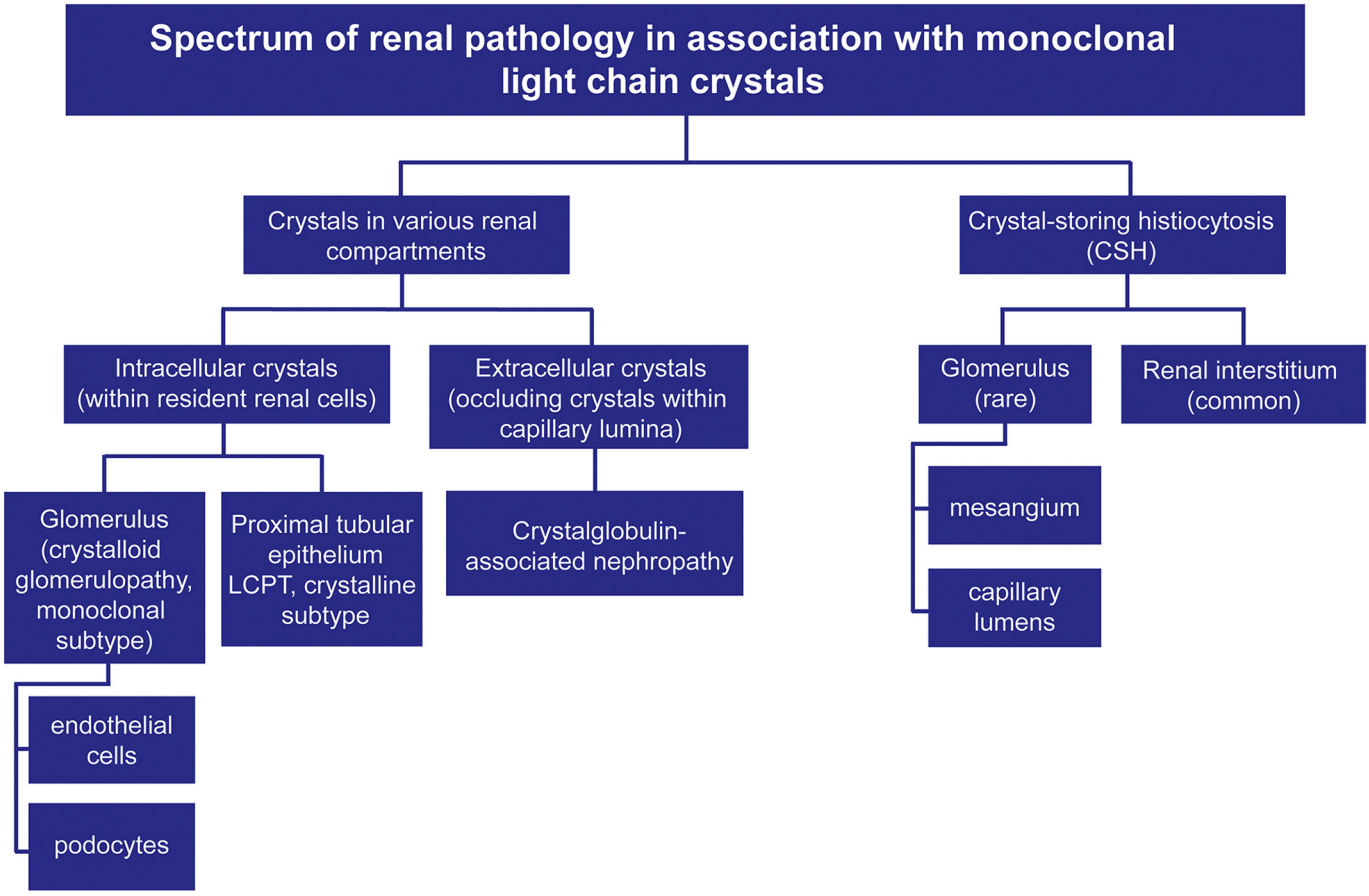

Fig. 5. Flowchart depicting the spectrum of kidney involvement with monoclonal crystals.

them from the true Gaucher cells seen in Gaucher's disease and pseudo-Gaucher cells sometimes seen in the bone marrow in chronic myeloid leukemia [2,5,24].

It should be noted that the term CSH with regards to kidney should be used only when crystals are found within histiocytes and not when *in situ* crystals are found within endogenous glomerular cells [25,26] or free within renal microvascular lumina [27] as outlined in Table 1 and emphasized by Hoelbeek et al. [22]. At the same time, it should be noted that in the kidney CSH is rarely a stand-alone pathology, and is in fact, often found co-existing with other morphologic forms of monoclonal renal disease (both crystal and non-crystal forms) – including light chain proximal tubulopathy or LCPT - usually crystalline subtype, crystalloid glomerulopathy or nephropathy, and cast nephropathy.

The crystals as described in the literature are commonly rhomboidal or needle-shaped and vary from being rarely electron-lucent to more commonly electron-dense structures, and often displaying a lattice-like substructure or periodicity [5,6,10,11]. While the crystals in our first case had a definite lattice configuration on EM, the crystals or crystalloids in cases 2 and 3 were quite unique in being round to oval structures without substructure or periodicity on EM. When crystals have such unusual configuration, immunoelectron microscopy can be very helpful to confirm their monoclonal nature [28]. Many of the EM descriptions in earlier literature also describe these crystals surrounded by a unit membrane, although such a description is lacking in later literature [7,10,11].

The pathogenesis of CSH *per se* and the pathogenesis behind the overwhelming involvement of kappa light chain in crystal formation as compared to lambda, are closely linked albeit separate processes. Regarding CSH, it has been hypothesized that either the crystal formation occurs mainly within the monoclonal marrow plasma cells and the histiocytes are bystanders ingesting either free crystals or crystal-laden dying plasma cells, subsequent to which these crystals are pooled within the histiocytes to form larger crystals, or alternatively, the abnormal kappa light chains are released by the plasma cells into the peripheral blood, ingested by macrophages into their phagosomes through endocytosis, then incorporated within their secondary lysosomes where they undergo further degradation and polymerization to form crystalline inclusions [6,7,20,29]. However, many believe that simple light chain overproduction is not sufficient for CSH and also does not fully explain why kappa light chain is the culprit in most cases. Unusual hydrophobic residues at the variable (V) domain of the kappa light chain at position 30 or unusual amino acid substitutions in the V region are believed to render the kappa crystals resistant to lysosomal degradation within the histiocytes or elsewhere [5,12,17,30,31].

In conclusion, we present three unique cases where the glomerular capillary loops, rather than the more commonly affected interstitium, were predominantly involved by collections of kappa-predominant crystal-storing histiocytes. As review of past literature and our current cases demonstrates, the clinical presentation of renal CSH can be varied and complex. Patients with monoclonal disease may present with only mild proteinuria along with slight renal dysfunction as evidenced by a minimal rise in serum creatinine, though the majority of cases show involvement of multiple compartments of the kidney. In these cases, identification of crystal-storing histiocytes in the kidney may serve as the only diagnostic clue to an underlying monoclonal disease, either a plasma cell dyscrasia (MGUS or frank myeloma) or a low-grade or very rarely, a high-grade B-cell lymphoma, with or without bone marrow involvement. Alternatively, there may be extreme accumulation of crystal-storing histiocytes involving multiple organs, in which the CSH process may exceed the actual myeloma disease burden, resulting in considerable morbidity and even mortality [4,5,12]. Interestingly, while not statistically significant, there appears to be a trend toward

greater renal dysfunction and higher proteinuria in patients with more interstitial burden of crystal-laden histiocytes than with predominantly glomerular involvement. Thus, in all monoclonal cases with renal symptoms, a kidney biopsy with reflex EM is very important for both diagnosis and prognosis of the patient.

Acknowledgements

We wish to thank Noralinda Viloria, BS, HTL (ASCP) for the gross renal biopsy core image for Case 1, and Edward Roberts, CEMT (USA) for his expert assistance with immunoelectron microscopy for Cases 1 and 2. The authors would also like to thank Dr. Hyung Min Lim for follow-up information on Case 3.

Declaration of competing interest

None.

Funding

This research did not receive any specific grant from funding agencies in the public, commercial, or not-for-profit sectors.

References

[1] Rajkumar SV, Dimopoulos MA, Palumbo A, et al. International Myeloma Working Group updated criteria for the diagnosis of multiple myeloma. Lancet Oncol 2014;15:e538–48. https://doi.org/10.1016/S1470-2045(14)70442-5.
[2] Bridoux F, Leung N, Hutchison CA, et al. Diagnosis of monoclonal gammopathy of renal significance. Kidney Int 2015;87:698–711. https://doi.org/10.1038/ki.2014.408.
[3] Sethi S, Rajkumar V, D'Agati VD. The complexity and heterogeneity of monoclonal immunoglobulin-associated renal diseases. J Am Soc Nephrol 2018;29:1810–23. https://doi.org/10.1681/ASN.2017121319.
[4] Jones D, Bhatia VK, Krausz T, Pinkus GS. Crystal-storing histiocytosis: a disorder occurring in plasmacytic tumors expressing immunoglobulin kappa light chain. Hum Pathol 1999;30:1441–8. https://doi.org/10.1016/s0046-8177(99)90166-1.
[5] Lebeau A, Zeindl-Eberhart E, Muller EC, et al. Generalized crystal-storing histiocytosis associated with monoclonal gammopathy: molecular analysis of a disorder with rapid clinical course and review of the literature. Blood 2002;100:1817–27.
[6] Terashima K, Takahashi K, Kojima M, et al. Kappa-type light chain crystal storage histiocytosis. Acta Pathol Jpn 1978;28:111–38. https://doi.org/10.1111/j.1440-1827.1978.tb01254.x.
[7] Takahashi K, Naito M, Takatsuki K, et al. Multiple myeloma, IgA kappa type, accompanying crystal-storing histiocytosis and amyloidosis. Acta Pathol Jpn 1987;37:141–54. https://doi.org/10.1111/j.1440-1827.1987.tb03142.x.
[8] Yamamoto T, Hishida A, Honda N, Ito I, Shirasawa H, Nagase M. Crystal-storing histiocytosis and crystalline tissue deposition in multiple myeloma. Arch Pathol Lab Med 1991;115:351–4.
[9] Arnold CA, Frankel WL, Guo L, et al. Crystal-storing histiocytosis in the stomach: a clue to subtle hematolymphoid malignancies. Am J Surg Pathol 2018;42(10):1317–24. https://doi.org/10.1097/PAS.0000000000001097.
[10] Carstens PH, Woo D. Crystalline glomerular inclusions in multiple myeloma. Am J Kidney Dis 1989;14:56–60.
[11] Garcia JF, Sanchez E, Lloret E, Martin J, Piris MA. Crystal-storing histiocytosis and immunocytoma associated with multifocal fibrosclerosis. Histopathology 1998;33:459–64. https://doi.org/10.1046/j.1365-2559.1998.00531.x.
[12] Sethi S, Cuiffo BP, Pinkus GS, Rennke HG. Crystal-storing histiocytosis involving the kidney in a low-grade B-cell lymphoproliferative disorder. Am J Kidney Dis 2002;39:183–8. https://doi.org/10.1053/ajkd.2002.29914.
[13] Tomioka M, Ueki K, Nakahashi H, et al. Widespread crystalline inclusions affecting podocytes, tubular cells and interstitial histiocytes in the myeloma kidney. Clin Nephrol 2004;62:229–33. https://doi.org/10.5414/CNP62229.
[14] Papla B, Spolnik P, Rzenno E, et al. Generalized crystal-storing histiocytosis as a presentation of multiple myeloma: a case with a possible pro-aggregation defect in the immunoglobulin heavy chain. Virchows Arch 2004;445:83–9. https://doi.org/10.1007/s00428-004-1031-3.
[15] Keller LS, Faull RJ, Smith P, et al. Crystalloid deposits in the kidney. Nephrology 2005;10:81–3. https://doi.org/10.1111/j.1440-1797.2005.00290.x.
[16] Tholouli E, Krebs M, Reeve R, Houghton JB. Crystal-storing histiocytosis in a patient with IgG kappa multiple myeloma. Br J Hematol 2005;128:412. https://doi.org/10.1111/j.1365-2141.2004.053.62.x.
[17] Stokes MB, Aronoff B, Siegel D, D'Agati VD. Dysproteinemia-related nephropathy associated with crystal-storing histiocytosis. Kidney Int 2006;70:597–602. https://doi.org/10.1038/sj.ki.5001524.
[18] Pitman SD, Wang J, Serros ER, Zuppan C. A 70-year old woman with acute renal failure. Arch Pathol Lab Med 2006;130:1077–8. https://doi.org/10.1043/1543-2165(2006)130[1077:AYWWAR]2.0.CO;2.
[19] Farooq U, Bayerl MG, Abendroth CS, Verma N, Talamo G. Renal crystal storing histiocytosis in a patient with multiple myeloma. Ann Hematol 2009;88:807–9. https://doi.org/10.1007/s00277-008-0660-z.
[20] El Hamel C, Thierry A, Trouillas P, et al. Crystal-storing histiocytosis with renal Fanconi syndrome: pathological and molecular characteristics compared with classical myeloma-associated Fanconi syndrome. Nephrol Dial Transplant 2010;25:2982–90. https://doi.org/10.1093/ndt/gfq129.
[21] Shah S, Sethi S, Arend L, Geetha D. Crystal-storing histiocytosis. Kidney Int 2016;89:507. https://doi.org/10.1016/j.kint.2015.12.012.
[22] Hoelbeek J, Duivenvoorden R, de Boer OJ, et al. Unique renal manifestations of type 1 cryoglobulinemia, with massive crystalloid deposits in glomerular histiocytes, podocytes, and endothelial cells. Am J Clin Pathol 2016;145:282–5. https://doi.org/10.1093/ajcp/aqv027.
[23] Wu C-K, Yang A-H, Lai H-C, Lin BS. Combined proximal tubulopathy, crystal-storing histiocytosis, and cast nephropathy in a patient with light chain multiple myeloma. BMC Nephrol 2017;18:170. https://doi.org/10.1186/s12882-017-0584-8.
[24] Schaefer HE. Gammopathy-related crystal-storing histiocytosis, pseudo- and pseudo-pseudo-Gaucher cells: critical commentary and mini-review. Pathol Res Pract 1996;192:1152–62. https://doi.org/10.1016/S0344-0338(96)80037-9.
[25] Vankalakunti M, Bonu R, Shetty S, Siddini V, Babu K, Ballal SH. Crystalloid glomerulopathy in monoclonal gammopathy of renal significance (MGRS). Clin Kidney J 2014;7:296–8. https://doi.org/10.1093/ckj/sfu025.
[26] Matsuyama N, Joh K, Yamaguchi Y, et al. Crystalline inclusions in the glomerular podocytes in a patient with benign monoclonal gammopathy and focal segmental glomerulosclerosis. Am J Kidney Dis 1994;23:859–65.
[27] Gupta V, El Ters M, Kashani K, Leung N, Nasr SH. Crystalglobulin-induced nephropathy. J Am Soc Nephrol 2015;26:525–9. https://doi.org/10.1681/ASN.2014050509.
[28] Herrera GA, Turbat-Herrera E. Ultrastructural immunolabeling in the diagnosis of monoclonal light-and heavy-chain-related renal diseases. Ultrastruct Pathol 2010;34:161–73. https://doi.org/10.3109/01913121003672873.
[29] Tan M, Epstein W. Polymer formation during the degradation of the human light chain and Bence-Jones proteins by an extract of the lysosomal fraction of normal human kidney. Immunochemistry 1972;9:9–16. https://doi.org/10.1016/0019-2791(72)90278-9.
[30] Aucouturier P, Bauwens M, Khamlichi AA, et al. Monoclonal Ig L chain and L chain V domain fragment crystallization in myeloma-associated Fanconi's syndrome. J Immunol 1993;150:3561–8.
[31] Leboulleux M, Lelogt B, Mougenot B, et al. Protease resistance and binding of Ig light chains in myeloma-associated tubulopathies. Kidney Int 1995;48:72–9. https://doi.org/10.1038/ki.1995.269.